A CAD BASED SIMULATION TOOL TO ESTIMATE ENERGY BALANCES OF DEVICE INTEGRATED PV SYSTEMS UNDER INDOOR IRRADIATION CONDITIONS

N.H. Reich, W.G.J.H.M. van Sark, E.A. Alsema[1]
H. de Wit & A.H.M.E. Reinders[2]

[1] Dept. of Science, Technology and Society, Copernicus Institute for Sustainable Development and Innovation, Utrecht University, Heidelberglaan 2, 3584 CS, Utrecht, the Netherlands, N.H.Reich@chem.uu.nl
[2]University of Twente, Enschede, The Netherlands

ABSTRACT: Computer Aided Design (CAD) is used for a variety of applications. Accordingly, current CAD software offers powerful rendering and ray-tracing features, alongside sophisticated graphical user interfaces. This makes it somewhat surprising that CAD embedded rendering is only used to render images, rather than that additional processing of the thereby obtained information is performed. In this paper, we demonstrate how spatial irradiation distributions incident onto PV geometries can be obtained from CAD embedded rendering. This is a very promising simulation approach for a variety of PV systems, because it allows for simulating irradiation properties for virtually all kinds of PV geometries, including three dimensional (3D) shapes. To this end, three different geometries and a device integrated PV (DIPV) product are modelled: a flat, two different bend and double-bend geometries and the PV-powered computer mouse "SoleMio", with a flat solar cell incorporated under a double-bend, transparent plastic cover. The software tools and scripts presented will allow for improved analysis of irradiation properties incident on complex solar cell geometries. Consequently, this contribution will be especially useful for energy balance estimations of device integrated PV (DIPV) used indoors.
Keywords: Design, Software, Simulation, Ray Tracing, Modelling, Energy Performance, Evaluation, DIPV

1 INTRODUCTION

Contemporary photovoltaic (PV) simulation tools are limited to the determination of the performance of flat PV cells and static situations of use, or static irradiation conditions, respectively. Thus, only PV products with a fixed, flat geometry can be modelled, and simulating the dynamics of fluctuating irradiance properties is virtually impossible. As just recently shown by a simulation tool incorporated into Computer Aided Design (CAD) software (named 3D-PV [1]), however, modelling of cumulative irradiance on curved PV areas as well as for dynamic use- and irradiance-scenarios is theoretically possible. The focus of 3D-PV, however, is to estimate shading effects, i.e., the determination of shadowing caused by objects in the surrounding of PV areas; a rendering technique denoted 'ambient occlusion'. Consequently, only a single irradiation distribution to model the specific heights of spatially resolved irradiance intensities were used (i.e., the CIE overcast sky condition and the corresponding solid-angle distribution). In this paper, we demonstrate the feasibility of exploiting the rendering and ray-tracing capabilities offered by CAD software using modelled solid-angle distributions of actual time course irradiation data, for the purpose of simulating PV power output in a further, separate step.

2 METHODOLOGY AND METHODS

2.1 Modelled 3D-shapes

For the purpose of demonstrating the utility of CAD based irradiation simulations, a range of different, relatively simple 3D-shapes have been chosen: flat, bend and double bend geometries (see Fig. 1). The bending radius of the single bend geometries has been chosen as 60, 120 and 180 degrees, and hemispheres (full and half flattened) are used as double-bend surfaces.

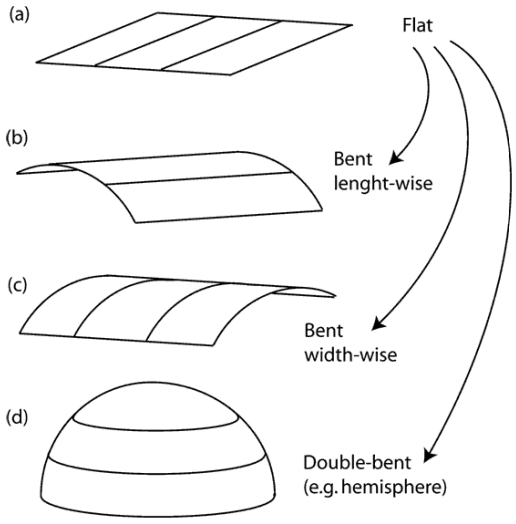

Figure 1: Modelled 3D-shapes used to demonstrate the utility of the CAD based PV simulation approach.

The orientation of the single bend geometries has been set such that the bending axis is oriented either parallel or perpendicular to a south facing direction. As solar cell interconnection, three cells of equal size are assumed to be series-connected (with cells aligned as shown in Fig. 1). As modelling PV power output is performed in an additional, further modelling step, it will not be discussed in detail in this paper. Here, the iPV-Sim tool [2], which in principle is suited for solving the two diode equation, was used for calculating short circuit current density yields, as elaborated in the results section.

2.2 Selecting 3D Studio Max (3DSM) as CAD software

The 3DSM CAD software offers a variety of powerful rendering and visualization features, illustrated in literature [3], making it a leading CAD program. However, the use of the specific 3DSM program for the purpose of this study was due to existing experience with the software and available, 3DSM specific "MAXscript" software code, as presented in [1], rather than that the 3DSM program was the resulting choice of a selection procedure. In fact, any 3D-CAD software theoretically allows for incorporating the presented results, as only the specific format of the software code is supposedly different. Here, it is interesting to note that a number of today's 3D-CAD tools incorporate the ray-tracer MentalRay [4], which also performs the rendering tasks presented here. Finally, it is worthwhile to note that 3DSM belongs to the Autodesk software environment, amongst other software offering the well-known program Auto-CAD.

2.3 General modelling approach

Three-dimensional (3D) rendering of solar radiation requires solid-angle irradiation distributions. Available irradiation data sets, however, are often limited to only global horizontal irradiation or direct and diffuse fractions, respectively. Therefore, we decided to distinguish the intended modelling tasks into three subsequent steps, with the first step being the determination of solid-angle distributions based on global horizontal irradiation data. This allows for using virtually any irradiation time series for the purpose of rendering irradiation distributions onto CAD modelled shapes, making it a very versatile simulation concept.

Once solid-angle distributions of irradiation are determined, rendering of irradiation incident onto the specific geometry is performed by 3DSM in a second, separate step. In the third, last step, the two-dimensional (2D) distributed irradiation incident onto the particular shape is translated into a 2D distributed photocurrent, generated by the solar cell assumed to be incorporated into that particular shape. The whole procedure is shown in Fig. 1.

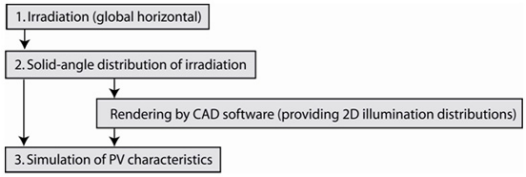

Figure 1: Three main "simulation-modules" used for simulating PV characteristics including CAD rendering.

In practice, however, a sheer infinite amount of possibilities exists to realize the modelling tasks shown in Fig. 1. The following therefore briefly describes the specific methods used and choices made.

2.3.1 Calculating solid angle distributions

The direct beam intensity together with a specific sun position as well as the diffuse fraction distribution is calculated based on CIE and Perez models [5] as well as sun position algorithms [6]. As irradiation data the STRANG web-interface [7] was used, which provides hourly averaged irradiation data distinguished into diffuse fractions of global horizontal irradiation and direct normal beam irradiation. Here, the best and worst days regarding overall daily irradiation sums during summer and winter solstices, respectively, for the location Utrecht, The Netherlands, have been used (see Table 1).

Table I: Overall global horizontal irradiation on days chosen to be modelled by hourly time-step simulations

Global horizontal irradiation [kWh/m2]	High	Low
Summer solstice	7.3	1.4
Winter solstice	0.9	0.2

The hourly averaged solar radiation time course data is translated into solid-angle resolved irradiation data in text-file format, providing the input for the actual rendering task performed by the 3DSM software. Note that the external software tool that realizes this modelling task is capable in providing any desired number of discrete sky-elements, which are used to describe a solid-angle distribution of irradiation. However, as a trade off between the computational performance of the CAD rendering task and the accuracy in output results we based modelling solid-angle distributions on 635 discrete elements.

2.3.2 CAD incorporated rendering

In order to model solid-angle irradiation distributions by 3DSM, 635 directional light-sources are arranged equidistantly over a hemisphere. Figure 2 shows a solid angle distribution using 635 light sources from within the 3DSM graphical user interface (GUI). Note that light sources in the front are not shown only for reasons of visibility and 3D perception, respectively.

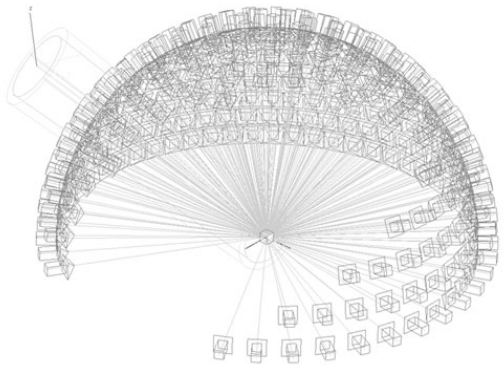

Figure 2: Example of a cut-out solid-angle distribution using 635 individual directional light sources in 3DSM.

In order to render the 2D irradiation distribution incident onto the concerned geometry, the render function "RenderToLightMap" is used. This results in externally saved bitmap images with Red-Green-Blue (RGB) color information representing specific irradiation intensities of each pixel of the CAD modelled shape.

2.3.3 Translating bitmap-colors into photocurrents

The bitmap images resulting from afore described rendering step are processed further to derive a

photocurrent, generated at a specific location (i.e., a specific pixel) of the modelled 3D-shape, using the equation normalized to the photocurrent density at full illumination:

$$J_{Ph} = J_{Ph,0} \cdot \frac{(1 - B + G + 3R - 2RG)}{4} \qquad (1)$$

In order to determine a specific PV power output, the specific solar cell geometries and the cell interconnection concept has to be clearly defined. Here, it is assumed that the irradiation intensity incident onto a single cell is the average of the irradiation intensity distribution incident onto that cell, using the 3D-shapes and cell alignments as described in sub-section 2.1.

2.4 A DIPV product example: The Sole Mio

The CAD based approach to eventually model PV power output is particularly interesting in the field of Device Integrated PV (DIPV) systems. The use of CAD incorporated PV simulation tools may allow product designers to instantly evaluate the energetic product performance throughout the ongoing design process. In addition to the geometries previously shown, we therefore also model a relatively complex geometry of a DIPV product: the PV powered computer mouse SoleMio, as presented in [8]. Here, it is assumed that the SoleMio is "sun-bathed" at a window sill location (see Fig. 3).

A two paned glazing system was incorporated by defining two transparent elements, having overall 80% transmission. Fresnel equations are incorporated into the MentalRay ray-tracer and are thus "automatically applied" to the defined refractive index, set to 1.5. This accounts for reflection at all four interfaces of the double paned glazing. In addition, the effect of lowered irradiation due to the transparent plastic cover of the SoleMio is analyzed. This is achieved by simply executing the rendering simulation with and without the transparent plastic cover attached to the PV mouse in the CAD drawing.

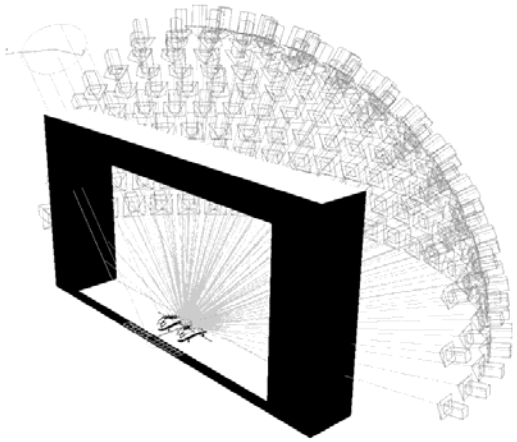

Figure 3: CAD modelled SoleMio at a window sill.

3 RESULTS

3.1 Irradiation incident onto 3D-shapes

The resulting, rendered bitmap images indicate a 2D distribution of irradiation intensity incident onto the specific geometry, be it the flat or a bend surface. Therefore, the 3D perspective of the 3D shapes is lost in the following pictures. However, from within the 3DSM GUI it is also possible to render the geometries having a 3D perspective, as shown in Fig. 4. Here, the resulting irradiation distributions for the best summer day at solar noon are shown.

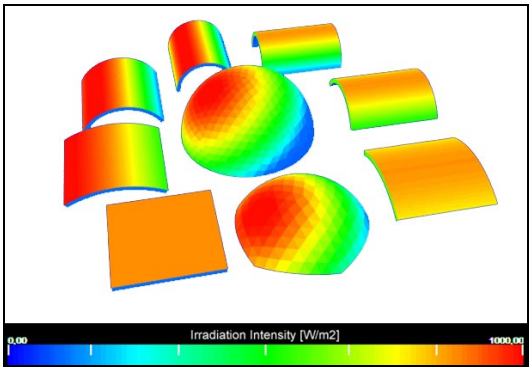

Figure 4: Rendered irradiance intensity distributions for the 3D-shapes viewed from within 3DSM GUI.

Figure 5 shows the resulting irradiation distributions incident onto a 120 degree, single bend shape, with the bending axis perpendicular to the south (solar noon, best summer day). Logically, the irradiation is distributed unequally only towards the direction perpendicular to the bend. This is very practical, as the irradiation distribution can be depicted in a 2D manner for single bend surfaces (i.e., in a "compressed" way).

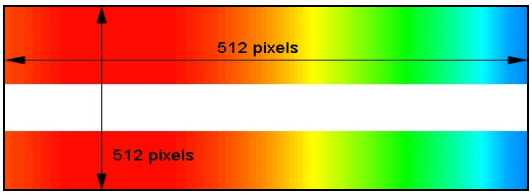

Figure 5: Irradiance distributions for a 120 degree single bend surface at solar noon.

The possibility to depict results of single bend surfaces in 2D is advantageous, also to show the effect of a different bending radius on irradiation distributions. Figures 6a through 6d show the resulting irradiance intensity distributions for the single bend surfaces numerically (with the bending axis perpendicular to the south), starting with zero bending (6a) and ending with a bending of 180 degrees (6d). The "compressed" way of showing the spatially resolved irradiation distribution is used to depict the change in irradiation intensity distributions incident onto that shape during the course of the day. To this end, Fig. 7 indicates the resulting distributions during the best summer day at summer solstice.

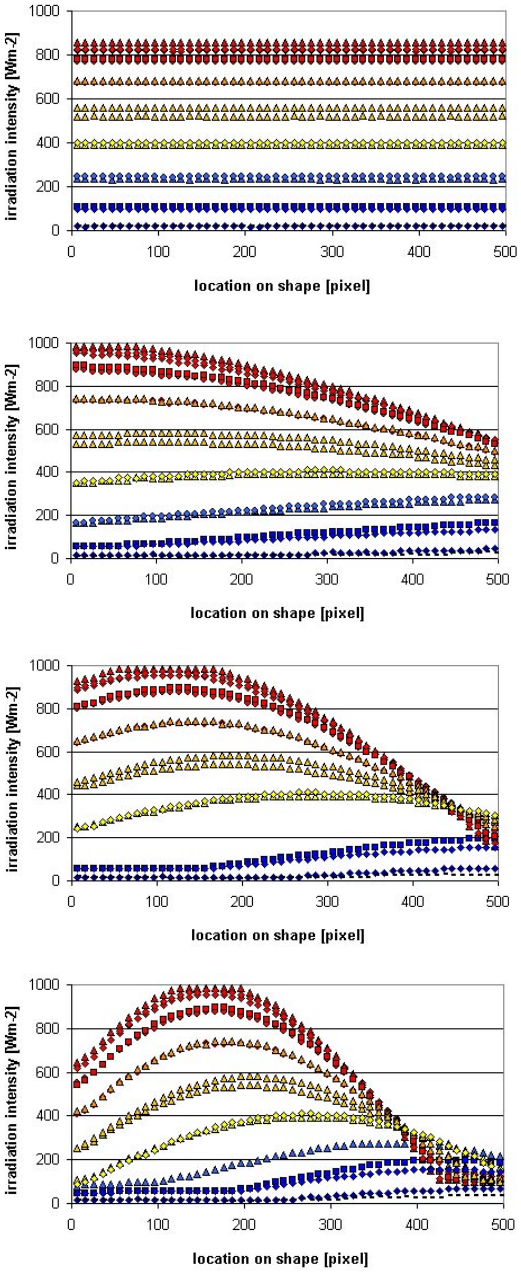

Figure 6a/b/c/d: Rendered intensity distributions for the single bend shapes with the bending axis perpendicular to a south facing direction during the best summer day.

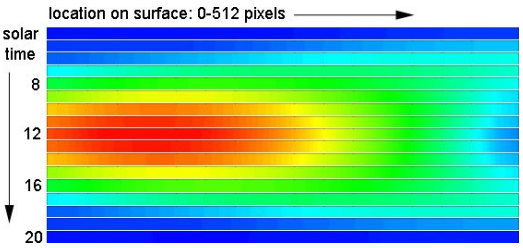

Figure 7: As in Fig. 5, but "compressed" into one day.

Obviously, the shape that has zero bending receives the actual global horizontal irradiation intensity, irrespective of the specific location of the shape (see flat lines in Fig. 7a). As global horizontal irradiation intensity was used as input (i.e., in step 1 described in section 2), the results shown in Fig. 7a) actually indicate the error range, which is caused from only computational processing. The resulting error is in the range of 1-2 W/m^2 (see small irregularities in Fig. 7a, which is attributed to the relatively huge amounts of data required to process (i.e., create and read) the bitmap images). Furthermore, a saturation effect can be identified (see Figures 7c and 7d). Here, irradiance intensity is obviously not larger than 1000 W/m^2, which can be related to the use of the normalized equation (similar to Eq. 1), defining maximum intensity H as 1000 W/m^2:

$$H = 1000 \cdot \frac{(1 - B + G + 3R - 2RG)}{4} \quad [W/m^2] \quad (2)$$

In general, the shown results clearly show that the larger the bend, the higher the spread in irradiation distributions at the specific surfaces. Consequently, achievable PV power output is affected to a larger extent towards a larger bend, as shown in the next sub-section.

3.2 Calculating a yield potential for 3D-shapes

For calculating actual PV yields (i.e., in energy units), specific weak light performances of cells have to be assumed, as presented in [9]. This would therefore assess the specific weak light performance of the specific solar cell chosen (i.e., the chosen diode parameter set), rather than that the effects of irradiation distributions onto the given 3D-shapes were in focus. Therefore, any detailed PV yield calculation is omitted. Instead, the resulting aggregated averages of short circuit current densities are calculated based on defined cell shape and cell arrangements (see section 2). As the least illuminated cell limits the short circuit current density of the other cells in series configuration, effects of the 2D irradiation distributions are thereby properly accounted for. Moreover, this approach also avoids the definition of an additional shunt resistance accounting for mismatch of cells (i.e., accounting for differing cell performances of interconnected cells). Thus, shading effects are accounted for, with the least illuminated cell limiting the short circuit current density of the other cells, whilst avoiding relatively complex solar cell performance modelling. For reasons of practicability we normalized the short circuit current density at one sun to 40mA/cm^2, and assumed surface areas of arbitrarily selected 1cm^2 for all shapes, so that the resulting aggregated and averaged short circuit current densities result in a short circuit current yield, as listed in Tables 3 through 6, in the unit mAh per day.

For easing comparisons, Table 2 lists irradiation sums (as already listed in Table 1), however, using the unit mWh/cm^2, which is much more practical regarding the chosen unit of the results (see Tables 3 through 6).

Table II: Overall global horizontal irradiation on days chosen to be modelled by hourly time-step simulations

Global horizontal irradiation [mWh/cm^2]	High	Low
Summer solstice	73	14
Winter solstice	9	2

Table III: Short circuit current yield potential of the flat geometry (in [mAh/d])

Geometry:	Summer		Winter	
	Best	Worst	Best	Worst
Flat	29	4	6	1

Table IV: Short circuit current yield potential of the single bend geometries, bending axis parallel to a south facing direction (in [mAh/d])

Geometry: Single bend	Summer		Winter	
	Best	Worst	Best	Worst
- 60 degrees	24	4	5	1
- 120 degrees	19	3	4	<1
- 180 degrees	11	3	3	<1

Table V: Short circuit current yield potential of the single bend geometries, bending axis perpendicular to a south facing direction (in [mAh/d])

Geometry: Single bend	Summer		Winter	
	Best	Worst	Best	Worst
- 60 degrees	27	4	4	1
- 120 degrees	22	3	4	<1
- 180 degrees	18	3	3	<1

Table VI: Short circuit current yield potential of hemispheres used to model double bend geometries (in [mAh/d])

Geometry: Hemisphere	Summer		Winter	
	Best	Worst	Best	Worst
Full	16	2	2	<1
Half flattened	21	3	3	<1

3.3 The SoleMio

Figure 8 shows a false color image of the specific "window sill" irradiation scenario, chosen to be modelled in section 2. The shown rendering is based on a solid-angle distribution at solar noon (best summer day), avoiding that the encasing shades the incorporated solar cell, in turn allowing for estimating the effects of the transparent plastic cover. Note the relatively high direct beam fraction $E_{dir,hor}$ = 720 W/m^2, which in conjunction with $E_{dif,hor}$ = 150 W/m^2 leads to a relatively large decrease in irradiance intensity that transmits through the cover to the cell by 12%.

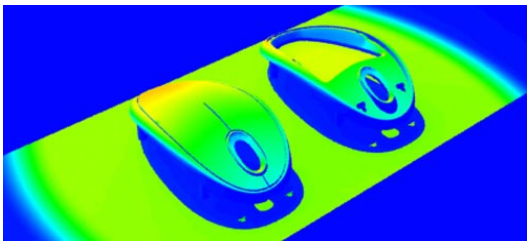

Figure 8: False color rendering of the SoleMio PV mice

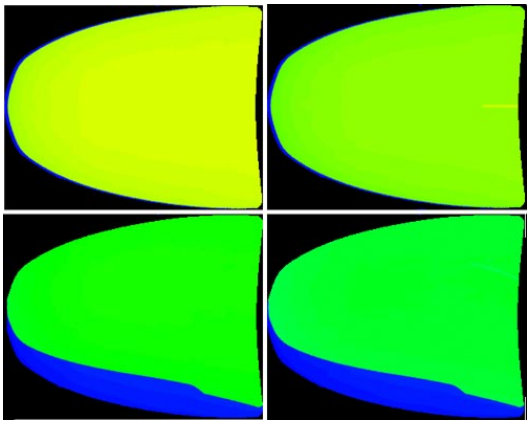

Figure 9: False color rendering of the flat, rigid solar cell incorporated into the SoleMio wireless PV mouse (on the left without and on the right with plastic cover attached).

Performing the same rendering simulation for the SoleMio, but for irradiation conditions three hour prior to the previously shown case, leads to an irradiance intensity decrease of only 0.7%, caused by the transparent plastic cover.

The respective images containing the RGB color information used to determine these figures are shown in Fig. 9 (with cover attached on images shown on the right hand side). Note that the shading effect in the lower images of Fig. 9 (i.e., solar noon minus three hours) is due to the SoleMio encasing, shadowing the cell area (see blue areas in Fig. 9), which is not included in above stated intensity decrease.

4 DISCUSSION

The previous results section and the shown irradiation distributions indicate that modelling irradiation intensity incident onto complex 3D shapes is relatively easy, using the presented, CAD based simulation approach. The major obstacle of CAD based simulations of irradiation conditions for PV systems, however, is that illumination and not irradiation is ray-traced: the photopic response curve of the human eye is inherently applied to the simulation algorithms rather than considering irradiance in the wavelength domain of the spectral response (SR) of the specific solar cell.

The lack of handling spectrally resolved irradiance requires the introduction of mismatch factors (MMF) to account for spectral effects. This is key, as otherwise tremendous differences result comparing CAD simulated PV power output with power output when simply matching wavelength resolved parameters of the involved components (i.e., SR of PV to solar spectra (e.g. AM1.5) and spectrally resolved glazing transmission characteristics).

Therefore, future CAD based PV simulation development should focus on incorporating simulation methods that account for spectral irradiance properties, i.e., accounting for the full spectral resolution applicable for PV technology rather than for the human eye.

5 CONCLUSIONS

We demonstrated a simulation concept that allows for using the powerful rendering and ray-tracing capabilities incorporated into state-of-the-art CAD software tools, for the purpose of simulating irradiation properties to be used for further PV simulation in a further, separate step. To this end, a bundle of three software tools and scripts are used together with the CAD software environment 3DSM. Aside of the detailed charge yields resulting for the specific geometries and cell-interconnections modelled, the results indicate that the presented simulation concept allows for relatively easily simulating irradiation distributions also for complex, three dimensional shapes.

However, the major obstacle of CAD based simulations of irradiation conditions for PV systems is found to be related to spectral effects: as the 3d-sm CAD environment inherently relates the photopic response curve to the calculation algorithms of the ray-tracer (i.e., illumination intensity distributions in LUX are inherently used), no information on the spectral composition of incident irradiance is available.

Nonetheless, we suggest that the demonstrated irradiance simulation tool may actually be key in future PV simulation programs: Particularly as CAD software may function as a software link between computer tools that model wavelength resolved solar radiation (i.e., SPECTRL2, MODTRAN, etc.) and solar cell device structures (i.e., PC1D, SCAPS, Afors-HET, etc.), based on physical properties. However, for this, of course a tremendous amount of future research and particularly programming effort will be required. Nonetheless, it is exactly the tremendous amount of programming effort already incorporated in the ready available CAD software environments, from which future PV simulation platforms may benefit, i.e., the CAD tools themselves do not need to be re-invented.

ACKNOWLEDGEMENTS

Parts of this work were financially supported by the NWO-SenterNovem Energy Research programme.

REFERENCES

[1] A.H.M.E. Reinders: “A design method to assess the accessibility of light on PV cells in an arbitrary geometry by means of ambient occlusion”, in: Proceedings of 22nd European Photovoltaic Solar Energy Conference, Milan, Italy, 2007

[2] N.H. Reich, E.A. Alsema, W.G.J.H.M. van Sark: “iPV-Sim: A simulation tool for PV powered consumer systems“, in: Proceedings of the 21st European Photovoltaic Solar Energy Conference, (Eds. J. Poortmans, H. Ossenbrink, E. Dunlop, P. Helm), WIP-Renewable Energies, Munich, Germany, 2006, pp. 2301-2305.

[3] K. L. Murdock “3ds Max 2009 bible”, Wiley (2008)

[4] T. Driemeyer: “Rendering with mental ray”, Volume I, Second, revised edition, Springer Verlag Wien New York (2001)

[5] R. Perez, R. Seals, P. Ineichen, R. Steward and D. Menicucci: “A new simplified version of the Perez diffuse irradiance model for tilted surfaces”, *Solar Energy* **39** (3) (1987), pp. 221–231

[6] R. Grena: “An algorithm for the computation of the solar position”, *Solar Energy* **82** (5) (2008), pp. 462-470.

[7] STRANG irradiation data web-service, last accessed on 04.09.2008: http://produkter.smhi.se/strang/

[8] N.H. Reich, M. Veefkind, W.G.J.H.M. van Sark, E.A. Alsema, W.C. Turkenburg, S. Silvester: “A solar powered wireless computer mouse: Industrial design concepts”, *Solar Energy* (accepted for publication)

[9] N.H.Reich, W.G.J.H.M. van Sark, E.A. Alsema, S.Y. Kan, S. Silvester, A.S.H. van der Heide, R.W. Lof, R.E.I. Schropp: “Weak light performance and spectral response of different solar cell types”, Proceedings 20th European Photovoltaic Solar Energy Conference (2005), pp. 2120-2123